0026-895X/08/7402-403–412$20.00
MOLECULAR PHARMACOLOGY
Copyright © 2008 The American Society for Pharmacology and Experimental Therapeutics
Mol Pharmacol 74:403–412, 2008

Vol. 74, No. 2
44826/3362474
Printed in U.S.A.

Adipose Fibroblast Growth Factor 21 Is Up-Regulated by Peroxisome Proliferator-Activated Receptor γ and Altered Metabolic States

Eric S. Muise, Barbara Azzolina, David W. Kuo, Mohamed El-Sherbeini, Yejun Tan, Xiling Yuan, James Mu, John R. Thompson, Joel P. Berger, and Kenny K. Wong

Departments of Molecular Profiling (E.S.M, J.R.T, K.K.W) and Metabolic Disorders (B.A., D.W.K., M.E.-S., X.Y., J.M., J.P.B.), Merck Research Laboratories, Rahway, New Jersey; and Department of Informatics, Rosetta Inpharmatics LLC, Seattle, Washington (Y.T.)

Received January 16, 2008; accepted May 7, 2008

ABSTRACT

Adipose tissue is a metabolically responsive endocrine organ that secretes a myriad of adipokines. Antidiabetic drugs such as peroxisome proliferator-activated receptor (PPAR) γ agonists target adipose tissue gene expression and correct hyperglycemia via whole-body insulin sensitization. The mechanism by which altered gene expression in adipose tissue affects liver and muscle insulin sensitivity (and thus glucose homeostasis) is not fully understood. One possible mechanism involves the alteration in adipokine secretion, in particular the up-regulation of secreted factors that increase whole-body insulin sensitivity. Here, we report the use of transcriptional profiling to identify genes encoding for secreted proteins the expression of which is regulated by PPARγ agonists. Of the 379 genes robustly regulated by two structurally distinct PPARγ agonists in the epididymal white adipose tissue (EWAT) of db/db mice, 33 encoded for known secreted proteins, one of which was FGF21. Although FGF21 was recently reported to be up-regulated in cultured adipocytes by PPARγ agonists and in liver by PPARα agonists and induction of ketotic states, we demonstrate that the protein is transcriptionally up-regulated in adipose tissue in vivo by PPARγ agonist treatment and under a variety of physiological conditions, including fasting and high fat diet feeding. In addition, we found that circulating levels of FGF21 protein were increased upon treatment with PPARγ agonists and under ketogenic states. These results suggest a role for FGF21 in mediating the antidiabetic activities of PPARγ agonists.

The prevalence of type 2 diabetes mellitus worldwide was estimated to be 170 million people in 2000, and this figure is expected to increase to more than 360 million by 2030 (Wild et al., 2004). Current therapies for diabetes include the insulin sensitizers rosiglitazone and pioglitazone, both agonists of the PPARγ nuclear receptor. Upon target engagement with these agonists, PPARγ changes conformation and induces transcription of its downstream target genes. PPARγ regulates genes involved in adipocyte differentiation, lipid synthesis and storage, insulin signaling, and glucose metabolism (Berger et al., 2005). Activation of PPARγ also leads to the secretion of adipokines that are implicated in whole-body insulin sensitization. One well studied secreted factor is adiponectin, which has been suggested to play a significant role in the efficacy of PPARγ agonists (Nawrocki et al., 2006). Originally identified in mature 3T3-L1 adipocytes (Scherer et al., 1995) and subsequently demonstrated to be regulated by PPARγ (Nawrocki et al., 2006), adiponectin is highly up-regulated during adipogenesis and secreted into the circulation. Data support adiponectin as a liver- and muscle-directed adipokine that improves glucose tolerance via activation of 5′-AMP-activated protein kinase (Nawrocki et al., 2006). In addition to adiponectin, PPARγ can regulate other secreted factors (e.g., resistin) that could contribute to the antidiabetic effects of these agonists (Steppan et al., 2001). The broad transcriptional affects of PPARγ activation warrants a systematic approach to identify downstream secreted factors that would aid in a better understanding of the mechanism of action. To this end, several approaches have been reported (Klimcakova et al., 2007; Lecka-Czernik et al.,

E.S.M. and B.A. contributed equally to this work.

Article, publication date, and citation information can be found at http://molpharm.aspetjournals.org.
doi:10.1124/mol.108.044826.

ABBREVIATIONS: PPAR, peroxisome proliferator-activated receptor; EWAT, epididymal white adipose tissue; WY14643, 4-chloro-6-(2,3-xylidino)-2-pyrimidinylthioacetic acid; COOH, 2-(2-(4-phenoxy-2-propylphenoxy)ethyl)indole-5-acetic acid; KO, knockout; IWAT, inguinal white adipose tissue; PAGE, polyacrylamide gel electrophoresis; PBS, phosphate-buffered saline.

2007). Klimcakova et al. (2007), using antibody arrays, reported that PPARγ treatment decreased leptin and IL-6 protein levels secreted in the media of cultured human adipose explants. Lecks-Czernik et al. (2007), using transcriptional profiling, identified several members of the IGF protein family and receptors to be regulated by PPARγ in vitro. Although Lecka-Czernik et al. (2007) conducted a genome scale transcriptional survey of PPARγ gene regulation, the data analysis was not focused specifically in identifying novel secreted factors regulated by PPARγ. Furthermore, the transcriptional profiling study was performed in the context of bone marrow stromal/stem cells during in vitro differentiation into adipocytes.

The goal of the current study was to systematically identify potential secreted proteins regulated by PPARγ in an animal model of diabetes using transcriptional profiling. We report the identification of 33 genes, coding for secreted proteins, robustly regulated by PPARγ agonists in epididymal white adipose tissue (EWAT) of db/db mice, one of which was FGF21. Some of these have been previously reported to be regulated by PPARγ, whereas others have not, although some have been implicated in metabolic processes. It is noteworthy that expression of FGF21 in vivo was found to be regulated by PPARγ, suggesting a role for this protein in mediating the antidiabetic activities of PPARγ agonists.

Materials and Methods

Compounds. Rosiglitazone (5-(4-{2-[methyl(pyridin-2-yl)amino]-ethoxy}benzyl)-1,3-thiazolidine-2,4-dione); the nonthiazolidinedione PPARγ agonist, COOH [2-(2-(4-phenoxy-2-propylphenoxy)ethyl)-indole-5-acetic acid (Carley et al., 2004; Laplante et al., 2006)]; and fenofibrate (2-[4-(4-chlorobenzoyl)phenoxy]-2-methylpropanoic acid isopropyl ester) were synthesized by Merck Research Laboratory chemists. WY14643 was purchased from Chemsyn.

In Vivo Treatments for Transcriptional Profiling. All animal experiments and euthanasia protocols were conducted in strict accordance with the National Research Council's *Guide for the Care and Use of Laboratory Animals*. Animal experiment protocols were reviewed and approved by the Institutional Animal Care and Use Committee of Merck Research Laboratories. The laboratory animal facilities of Merck Research Laboratories are certified by the Association for Assessment and Accreditation of Laboratory Animal Care International. Animals were housed in temperature-, humidity-, and light-controlled rooms (21–23°C, 47–65%, 12–12 h light/dark cycle, respectively). All animals were male and were euthanized by CO_2 asphyxiation 6 h after the final dose (for drug treatments) and the tissues were harvested and flash-frozen in liquid nitrogen. Drug dosing was performed once daily in the morning by oral gavage for the number of days indicated.

db/db mice (lpr−/−, 10 weeks old, $n = 3$ per treatment group; Charles River Laboratories, Wilmington, MA) were housed eight animals per cage, provided food (LabDiet 5001; Purina St. Louis, MO) and water ad libitum, and dosed with vehicle (0.25% methylcellulose), rosiglitazone (30 mg/kg), or COOH [30 mg/kg (Carley et al., 2004; Laplante et al., 2006)] for 8 days (efficacious doses). Fasting tail-nick blood samples were collected 1 day before the start of dosing and 1 day after the last dose and plasma concentrations of glucose were determined (glucose Trinder assay kit; Sigma, St. Louis, MO). For serum FGF21 protein determination, 7-week-old animals were dosed once daily in the morning by oral gavage with vehicle (0.25% methylcellulose) or rosiglitazone (10 or 30 mg/kg) for 14 days.

To delineate the role of PPARα in the regulation of FGF21, PPARα KO mice [129Sv background; $n = 3$ per treatment group; Taconic Farms, Germantown, NY (Lee et al., 1995)] or their wild-type littermates were dosed with vehicle (0.25% methylcellulose), rosiglitazone (100 mg/kg), or fenofibrate (200 mg/kg) for 7 days. Doses were chosen to ensure maximal receptor engagement because these animals were normoglycemic. PPARγ KO mice were unavailable because of the embryonic lethality of the mutation.

To demonstrate FGF21 regulation by different PPAR agonists across multiple mouse models and fat depots, two additional strains (lean CD1 and C57BL/6) and a second fat depot (inguinal white adipose tissue, IWAT) were tested. CD1 mice (11 weeks old, $n = 3$ per treatment group; Charles River Laboratories) were dosed with vehicle (0.25% methylcellulose), rosiglitazone (100 mg/kg), or fenofibrate (300 mg/kg) for 14 days, whereas C57BL/6 mice (9–11 weeks old, $n = 3$ per treatment group; Charles River Laboratories) were fed standard rodent chow and were dosed with either vehicle (0.25% methylcellulose), the PPARα agonist WY14643 (30 mg/kg), or rosiglitazone (100 mg/kg) for 7 days. Doses were chosen to ensure maximal receptor engagement because these animals were normoglycemic. To determine the effects of ketogenic conditions on FGF21 expression, a second group of C57BL/6 mice ($n = 4$ per treatment group; Taconic Farms) were fed chow diet (LM-485 mouse/rat sterilizable diet; Harlan Teklad, Madison, WI) until 5 weeks of age, then either kept on chow diet or switched to a high-fat diet [DIO (VHFD) 60 kcal% fat; Research Diets, New Brunswick, NJ] for 10 weeks. A group of at least five mice on chow diet were fasted for 24 h before tissue harvest.

In Vitro Treatments for Transcriptional Profiling. 3T3-L1 cells were grown to confluence in medium A (Dulbecco's modified Eagle's medium with 10% fetal calf serum, 100 units/ml penicillin, and 100 μg/ml streptomycin) at 37°C in 5% CO_2 and induced to differentiate as described previously (Zhang et al., 1996). In brief, differentiation was induced by incubating the cells with medium A supplemented with 3-isobutyl-1-methylxanthine, dexamethasone, and insulin for 2 days, followed by 2 days' incubation with medium A supplemented with insulin. The cells were further incubated in medium A for an additional 4 days to complete the adipocyte conversion. At day 8 after the initiation of differentiation, cells were incubated in medium A plus or minus compounds for 24 h at saturating concentrations: vehicle (0.1% dimethyl sulfoxide), rosiglitazone (10 μM), or COOH (10 μM).

RNA Isolation from Tissues and Cells. Total RNA was isolated from frozen tissues after homogenizing in UltraSpec RNA reagent (Biotecx Laboratories, Inc., Houston, TX) or TRIzol reagent (Invitrogen, Carlsbad, CA) with a PT 10/35 Polytron (Kinematica Inc., Bohemia, NY) and processed using RNeasy kits (QIAGEN, Valencia, CA) according to the manufacturers' instructions. For 3T3-L1 adipocytes, total RNA was prepared using TRIzol reagent (Invitrogen) and RNeasy kits (QIAGEN). RNA concentrations were estimated from absorbance at 260 nm.

Microarray Analysis. Microarray processing was performed as described previously (Hughes et al., 2001). In brief, labeled cRNA was hybridized for 48 h onto 60-mer two-color spotted microarrays (Agilent Technologies, Santa Clara, CA). Individual treatment samples (including individual vehicle treatment samples) were hybridized against a vehicle treatment pool. LogRatio and P values were generated by averaging replicates (3–5 replicates per treatment) and using the AHEM algorithm in the Rosetta Resolver version 6.0 software (Rosetta Inpharmatics LLC, Seattle, WA). LogRatio values represent the difference in regulation of the compound treated samples versus the vehicle-treated sample, where a positive value signifies up-regulation after compound treatment and a negative value signifies down-regulation after compound treatment. Genes coding for secreted proteins were identified using keyword searches such as "secreted" and "extracellular" from the SwissProt, TrEMBL, and Proteome databases.

Cloning of FGF21 into The Yeast Expression Vector pPICZαB. The mouse FGF21 cDNA was cloned into the pPICZαB vector by polymerase chain reaction from liver cDNA using standard molecular biology techniques and the primers 5′-CTC-

GAGAAAAGATACCCCATCCCTGACTCCAGCCCCCTCCTC-3′ (sense) and 5′-GCGGCCGCTCACTTGTCATCGTCGTCCTTGTAATCGGACGCATAGCTGGGGCTTCGGCCCTGT-3′ (antisense). A FLAG tag sequence was introduced at the 3′ end.

Expression and Purification of Recombinant FGF21. The recombinant plasmid pPICZα-FGF21 was linearized with SalI to favor the integration at the *his*4 locus of *Pichia pastoris* genome and transformed into yeast by electroporation. Transformants were selected by incubation at 30°C for 2 to 3 days on yeast extract/peptone/glucose agar plates containing 100 μg/ml Zeocin. A total of 16 Zeocin-resistant colonies were analyzed for production of FGF21 through small scale expression trials in 10 ml of buffered minimal glycerol-complex medium. The cultures were incubated at 30°C until they reached OD_{600} = 2 (approximately 24 h). Subsequently, the cells were pelleted by centrifugation (3000*g* for 5 min) and resuspended in 2 ml of buffered minimal methanol-complex medium for induction of the AOX I promoter. For expression of FGF21, methanol was added to the culture every 24 h at a final concentration of 0.5%, and incubation was carried out at 30°C for 3 days with vigorous shaking. The culture medium was cleared of yeast cells by centrifugation at 3000*g* for 10 min. Presence of recombinant FLAG-tagged FGF21 in the culture media was monitored by SDS-PAGE followed by silver staining and by Western blot analysis using anti-FLAG antibodies. The estimated full-length protein yield was 1 mg/ml of media. A yeast clone producing a protein species of the same size as FGF21 was chosen for large-scale production, where the volume of growth medium was increased to 1000 ml. The purification procedure was as described above for small-scale production but increased proportionately.

FGF21 was purified via affinity column chromatography using anti-FLAG M2 monoclonal antibody affinity gel (Sigma) from the media containing secreted recombinant FLAG-tagged mouse FGF21. Fractions were eluted with 250 μg/ml FLAG peptide. The majority of the purified protein eluted in fraction 2. The peak fractions were concentrated using the Biomax-5 ultrafiltration device (Millipore, Billerica, MA) and washed three times with PBS to remove any residual peptide. Final protein concentration was determined using BCA protein assay (Pierce, Rockford, IL) according to the manufacturers' instructions, using bovine serum albumin protein dilutions for standard curve.

Generation of Antipeptide Antibodies. Three different antigenic peptides were identified, synthesized and conjugated with keyhole limpet hemocyanin (GGQVRQRYLYTDDDQ = peptide A; LEDGYNVYQSEAHG = peptide B; and LPPEPPDVGSSDPL = peptide C). They were used in combination to challenge rabbits (Covance Research Products, Princeton, NJ). The antisera were tested by enzyme-linked immunosorbent assay (Covance Research Products) with each antigenic peptide to give the individual relative antigenic response.

Evaluation of Mouse Plasma/Serum and Sample Preparation. Approximately 1 ml of whole blood was removed via cardiac puncture and immediately aliquoted into two 500-μl Microtainer tubes with EDTA (BD Biosciences, San Jose, CA) and mixed by slow inversion. The blood samples were then spun in a Hermle refrigerated microcentrifuge (with adapters; MIDSCI, St. Louis, MO) for 5 min at 14,000 rpm at 4°C. The supernatant (plasma) was removed carefully and aliquoted into 1.5-ml Eppendorf tubes and flash-frozen in liquid nitrogen. Approximately 250 to 300 μl of plasma per animal was collected by this method. To load the maximum volume of plasma/serum on the gel, albumin was depleted using the Cibacron Blue spin column albumin removal kit from Genomic Solutions, Inc (Ann Arbor, MI). Fifty microliters of serum was diluted to 200 μl with binding buffer provided and passed over the column. The albumin-depleted serum was passed over a second time, and this 200 μl of diluted serum was mixed with 5× sample buffer (250 mM Tris, pH 6.8, 10% SDS, 0.5% bromphenol blue, 50% glycerol, and 100 mM β-mercaptoethanol). An aliquot of 30 μl was boiled for 25 min, and 25 μl of boiling sample was loaded onto a 10 to 20% acrylamide gel for Western blot analysis.

Quantitative Western Blot Analysis. Protein samples were separated on SDS-PAGE 10 to 20% gradient gels (Ready gel; Bio-Rad Laboratories, Hercules, CA) and were transferred to nitrocellulose (0.2 μm pore size; Invitrogen) using the Bio-Rad Western transfer unit. The membranes were blocked in 3% skim milk in PBS at 4°C overnight. Blocking solution was replaced with fresh blocking solution containing 0.1% Tween 20 and antisera at the appropriate dilution. Blots were incubated at room temperature with shaking for 2 h. The membranes were rinsed in water several times and washed four times with PBS + 0.1% Tween 20 for a total of 2 h. Secondary antibody (IR Dye 800 conjugated anti-rabbit IgG from Rockland Immunochemicals (Gilbertsville, PA) was incubated with the membranes at a dilution of 1:5000 in blocking buffer + 0.1% Tween 20. Blots were incubated at room temperature with shaking for 45 min, covered with aluminum foil. All procedures from this step forward were kept covered to protect the blot from light. The secondary antibody was removed and filters were washed three times in PBS + 0.1% Tween 20 with water rinses in between. The blots were then washed in PBS (no Tween) for a final wash. The filters were scanned on the Odyssey Infrared Imaging system by LI-COR (Lincoln, NE). Blots were analyzed using Odyssey Application software and interfaced with Excel software (Microsoft Corp., Redmond, WA). Statistical analysis was performed using Excel and the Student's *t* test (two-sample, two-tail) to determine whether there were significant differences between the diets. Data were expressed as mean ± S.D. Purified recombinant mouse FGF21 was used as standard to quantitate plasma levels of FGF21.

Determination of Specific Bands by Peptide Blocking. Plasma samples have several bands that are visible after developing with antibody. Evaluation of albumin depleted db/db mouse plasma by Western blot was compared with blots developed using prebleed (naive) antisera from the same rabbit (MS2692) that was later challenged with three peptide antigens. Specificity was verified by peptide blocking using a mixture of the three peptides used to challenge the rabbit. In two separate tubes, 10 μl of antiserum from MS2692 were added. To one of the tubes, 100 μg of peptide A, 100 μg of peptide B, and 50 μg of peptide C were added in a total of 250 μl of PBS. To the other tube, 250 μl of PBS was added. Both tubes were incubated at 37°C for 1 h and then 4°C overnight. Both tubes were centrifuged at 11,000 rpm for 15 min at 4°C. The supernatants were diluted to 10 ml in 3% milk powder and 0.2% Tween 20 in PBS. This was used as antisera for duplicate Western blots. Blots were developed as described under *Quantitative Western Blot Analysis*.

Results

Identification of Genes Encoding for Secreted Proteins Regulated by PPARγ Agonists in Adipose Tissue. To identify novel secreted proteins regulated by PPARγ agonists, global gene expression profiling experiments were conducted in adipose tissue of diabetic db/db mice treated with either vehicle or one of two structurally different PPARγ agonists (rosiglitazone or COOH at 30 mg/kg) for 8 days. This treatment paradigm resulted in an improvement in plasma glucose level from approximately 450 mg/dl to approximately 150 mg/dl in these animals (data not shown). Analysis of EWAT gene expression identified 379 genes that were regulated at least 1.5-fold (with $p < 0.01$) by both PPARγ agonists (Fig. 1A), representing roughly a third of the total signatures of each compound in terms of number of probes meeting that cutoff (data not shown). Because of the significant structural differences between these two ligands, we believe that the intersection, using these cutoffs, represents a very robust PPARγ target gene signature (both directly and indirectly

regulated genes) in the adipose tissue. Of the 379 genes, 33 were annotated as coding for secreted proteins from public databases (see *Materials and Methods*) (Fig. 1B). A subset of the 33 genes has previously been shown to be regulated at the transcript level by PPARγ agonists [e.g., adiponectin (Adipoq; Combs et al., 2002), FGF21 (Fgf21; Wang et al., 2008), lipoprotein lipase (Lpl; Auwerx et al., 1996), Laminin b3 (Lamb3; Routh et al., 2002), and TNFα (Tnf; Singh Ahuja et al., 2001)] (Table 1). Adiponectin, FGF21, and lipoprotein lipase were up-regulated by PPARγ agonist treatment, whereas Laminin b3 and TNFα were down-regulated (Table 1). Adiponectin and TNFα are two well established proteins that oppositely regulate insulin sensitivity (Boyle, 2004). The expression profile in adipose tissue shows that in db/db mice, adiponectin mRNA is decreased 3.8-fold and TNFα is increased 1.7-fold compared with lean db/+ animals. Pharmacological treatment with PPARγ agonists increased adiponectin mRNA expression 2.7-fold and decreased TNFα expression 1.5-fold, consistent with their role in regulating insulin sensitization (Table 1). Adiponectin gene expression changes also translate into changes in plasma adiponectin, which is decreased in obese and diabetic humans and increased with PPARγ agonist treatment (Yu et al., 2002). Similar results have been reported in rodent models (Nawrocki et al., 2006).

Other genes identified here have been implicated in the diabetes phenotype [Retnla (Blagoev et al., 2002), IL13 (Kretowski et al., 2000), Sorbs1 (Kimura et al., 2001), Igf1 (Yakar et al., 2004), Npy (Woods et al., 1998)], in lipid metabolism [ApoC4 (Allan and Taylor, 1996), Angptl3 (Koishi et al., 2002)], and in the inflammatory response [Csf1 (Jadus et al., 1996), Ptpro (Teshima et al., 1998), Tnf (Hata et al., 2004), Ccl11 (Rokudai et al., 2006), Ccl8 (Heinemann et al., 2000), IL13 (Lloyd et al., 1997), Ccl12/Ccl2 (Moore et al., 2006), Ccl7 (Combadiere et al., 1995)]. Retnla, IL13, Sorbs1, Igf1, Apoc4, Angptl3, Ccl11, and Ccl8 were up-regulated in EWAT by PPARγ agonist treatment, whereas Npy, Csf1, Ptpro, Tnf, Ccl12/Ccl2, and Ccl7 were down-regulated (Table 1).

Other genes not previously associated with PPARγ agonist treatment were also identified; Fgf13, Postn, and Serpina3g mRNAs were up-regulated in EWAT by PPARγ agonist treatment, whereas Ctgf, Lox, Lfng, Wisp1, Timp1, Lrg1, Adamts, Wisp2, Hp, Tnc, and Ngp mRNAs were down-regulated (Table 1). Although the individual effects of modulating the expression levels of these genes is unknown at this time, collectively they must contribute to the biological activity of PPARγ agonists. Here, we focused on FGF21 for follow-up analysis as this protein has therapeutic potential to treat diabetes.

Recombinant FGF21 Expressed in *P. pastoris* and Production of anti-FGF21 Antibodies. Murine FGF21 was cloned and expressed in *P. pastoris* with a FLAG tag at its 3′-end. The protein was purified from the media using an anti-FLAG column and eluted with flag peptide (Fig. 2). This protein increased glucose uptake in 3T3-L1 adipoctyes (at 5 μg/ml) as reported previously (Kharitonenkov et al., 2005), but this activity was insulin-dependent (data not shown). To ascertain whether FGF21 was a circulating factor, polyclonal antibodies raised against 3 peptide sequences of FGF21 were used to detect circulating levels of this protein. The limit of

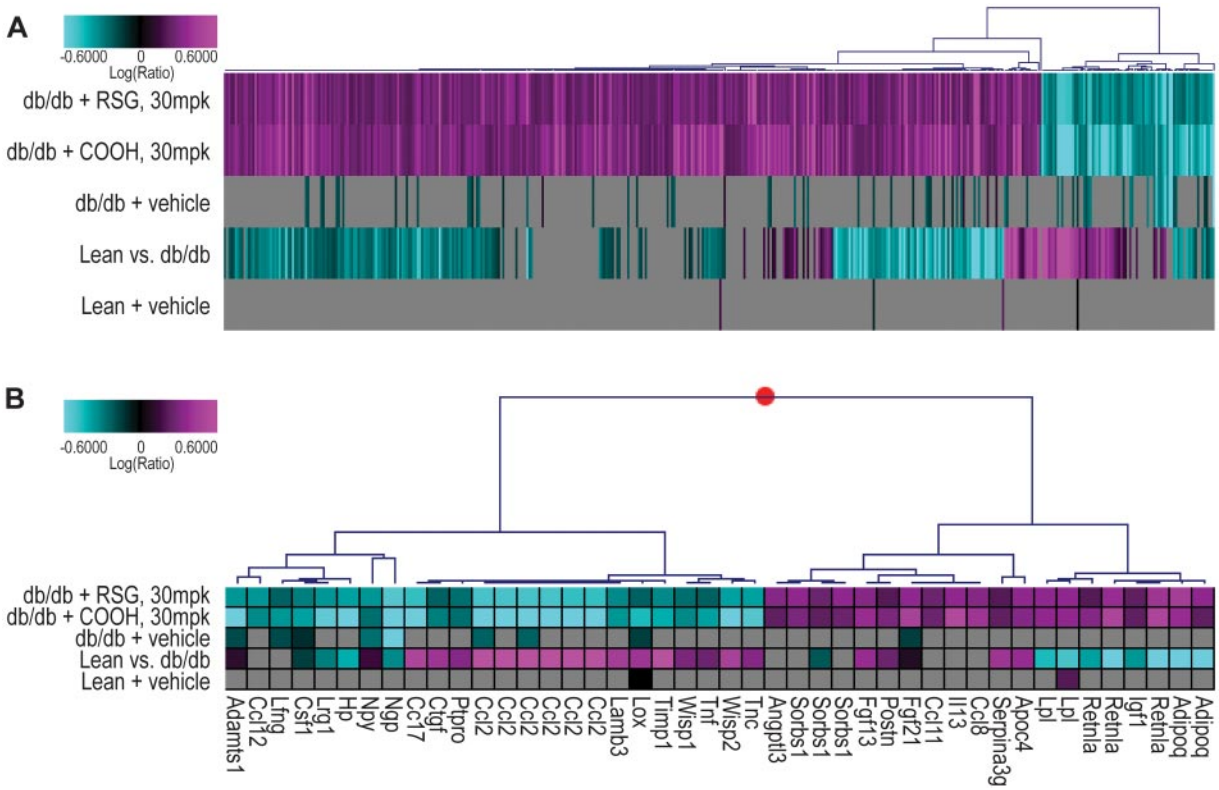

Fig. 1. PPARγ agonists alter the gene signature of db/db EWAT. Three hundred and seventy-nine genes were regulated by both rosiglitazone (RSG) and COOH at least 1.5-fold with $p < 0.01$ (represented by 452 probes on the array as shown in A). The regulation of these genes in db/db EWAT compared with lean EWAT is included (Lean versus db/db). Of these 379 PPARγ responsive genes, 33 code for known secreted proteins (represented by 44 probes on the array as shown in B). Shown are logRatio values colored magenta for up-regulation or cyan for down-regulation across a 4× range (± 0.6 logRatio). Data points with $p > 0.05$ are shaded gray.

TABLE 1

Thirty-three secreted proteins regulated by PPARγ agonists in adipose tissue of db/db mice

Shown are the mRNA ratio values obtained by Agilent microarray analysis for the 33 secreted proteins significantly regulated by both PPARγ agonists in EWAT of db/db mice.

Gene Name	Entrez ID	db/db+		Lean vs. db/db	Description
		Rosiglitazone (30 mg/kg)[a]	COOH (30 mg/kg)[a]		
Adipoq	11450	2.67	2.28	0.26*	Adiponectin, fat-derived hormone, modulates adipocyte differentiation, energy balance, proliferation, and insulin resistance
Retnla	57262	2.51	3.11	0.2*	Resistin like-α, an angiogenic and potent pulmonary vasoconstrictive protein that oligomerizes with resistin (Retn).
Fgf21	56636	2.23	2.83	1.14	Fibroblast growth factor 21, a member of the fibroblast growth factor family of secreted mitogens, strongly expressed in liver
Il13	16163	2.20	3.25	1.24	Interleukin 13, a cytokine that modulates B-cell IgE switching; human IL13 may be therapeutic for diabetes
Sorbs1	20411	2.18	1.89	0.84	Sorbin and SH3 domain containing 1 (ponsin), a likely SH3 adaptor involved in cell adhesion, glucose uptake, and insulin receptor signaling
Apoc4	11425	2.16	2.07	2.39*	Apolipoprotein C IV, an apolipoprotein C2-linked gene within an apolipoprotein gene cluster, expressed in the liver
Lpl	16956	2.14	2.13	0.34*	Lipoprotein lipase, hydrolyzes the triacylglycerol component of triacylglycerol-rich lipoproteins
Fgf13	14168	2.04	2.39	2.38*	Fibroblast growth factor 13, may play a role in heart development and nervous system development and function
Angptl3	30924	2.02	1.62	1.02	Angiopoietin-like 3, vascular endothelial growth factor family member, induces angiogenesis and regulates lipid metabolism
Ccl8	20307	1.99	2.55	1.20	Chemokine (C-C motif) ligand 8, induced after exposure to mycobacterial
Ccl11	20292	1.69	1.75	1.14	Chemokine (C-C motif) ligand 11 (eotaxin), a CC chemokine ligand for Ccr3, involved in eosinophil chemotaxis and extravasation
Igf1	16000	1.61	1.60	0.5*	Insulin-like growth factor 1, ligand for the protein tyrosine kinase-linked IGF receptor (Igf1r), stimulates cell proliferation
Postn	50706	1.53	1.83	1.72	Periostin osteoblast specific factor, cell adhesion molecule that is down-regulated by Wnt3 signaling
Serpina3g	20715	1.52	1.64	2.43*	Serine protease inhibitor 21 (α-1-antichymotrypsin-like protein), a member of the serpin family, inhibits cell growth
Tnf	21926	0.66	0.48	1.72*	Tumor necrosis factor, a macrophage-produced proinflammatory cytokine that mediates responses to bacteria and injury
Ctgf	14219	0.65	0.56	2.46*	Connective tissue growth factor, a putative insulin-like growth factor binding protein involved in angiogenesis, cell adhesion, cell migration, and ossification
Lox	16948	0.65	0.39	2.49*	Lysyl oxidase, enzyme that oxidizes lysine to α-aminoadipic-δ-semialdehyde in crosslinking of collagens and elastin, regulates Hras1
Lfng	16848	0.65	0.51	0.82	Lunatic fringe, a glycosyltransferase that modifies Notch receptors and thereby modulates signal transduction
Wisp1	22402	0.64	0.54	1.93*	Wnt1 inducible signaling pathway protein 1, promotes osteoblast differentiation and may act in bone repair, likely involved in Wnt1 signaling
Ptpro	19277	0.61	0.63	2.02*	Protein tyrosine phosphatase receptor type O, may be involved in the survival and differentiation or proliferation of macrophages
Csf1	12977	0.58	0.45	0.84*	Colony stimulating factor 1 (macrophage), regulates macrophage proliferation and differentiation, acts in bone development and reproduction
Timp1	21857	0.56	0.43	4.98*	Tissue inhibitor of metalloproteinase 1, inhibits matrix metalloproteases, contributes to anti-inflammatory responses
Lamb3	16780	0.55	0.50	2.69*	Laminin β 3, a subunit of laminin 5 that may be involved in hemidesmosome formation
Ccl12	20293	0.52	0.54	1.42	Chemokine (C-C motif) ligand 12, a chemoattractant for eosinophils and monocytes
Lrg1	76905	0.52	0.31	0.56*	Leucine-rich α-2-glycoprotein 1 (leucine-rich HEV glycoprotein), binds ECM proteins expressed on the basal lamina, such as fibronectin, collagen IV, laminin, and transforming growth factor-β
Npy	109648	0.51	0.61	1.32*	Preproneuropeptide Y, signals through G protein-coupled receptors to regulate food intake, bone formation, angiogenesis, nociception, and behavior and may function in lipid metabolism
Adamts1	11504	0.49	0.27	1.18	ADAM metallopeptidase with thrombospondin type 1 motif 1, regulates keratinocyte differentiation and cell migration
Wisp2	22403	0.48	0.19	2.9*	Wnt1 inducible signaling pathway protein 2, a member of the CCN family of growth factors
Hp	15439	0.48	0.20	0.44*	Haptoglobin, an acute phase protein that binds hemoglobin; rat Hp associates with abnormal β chain N-linked oligosaccharides in diabetic rats
Tnc	21923	0.45	0.33	2.06*	Tenascin C (hexabrachion), a multidomain extracellular matrix glycoprotein with epidermal growth factor-like and fibronectin type III-like repeats
Ccl7	20306	0.38	0.21	3.06*	Chemokine (C-C motif) ligand 7, linked to experimental asthma and experimental allergic encephalomyelitis
Ccl2	20296	0.34	0.21	6.59*	Chemokine (C-C motif) ligand 2, Ccr2 ligand that recruits leukocytes, acts in experimental allergic encephalomyelitis, rheumatoid arthritis and atherosclerosis
Ngp	18054	0.32	0.26	0.54*	Neutrophilic granule protein, a myeloid-specific protein that has similarity to the cysteine protease inhibitor cathelin

[a] All have $P < 0.01$.
* $P < 0.01$

detection for the FGF21 antibodies was 5 ng/ml determined by quantitative Western Blot analysis using recombinant *P. pastoris*-expressed protein as a standard. Endogenous levels of FGF21 protein in db/db plasma were detected and estimated at approximately 100 ng/ml. An expected band at 23 kDa was visible from db/db mouse plasma, and this was blocked by preincubating the antibody with peptide. This endogenous band migrated close to the recombinant FGF21 protein. A higher molecular mass band at 30 kDa was observed that was also blocked by peptide (Fig. 3). This extra band could represent a longer transcript (alternative start site), a higher molecular mass protein complex, or cross-reactivity to a related or unrelated protein. The peptides did not match any other mouse protein by BLAST search, however, and we could not identify a different start site or alternative transcript within the genomic region of *Fgf21*. Additional studies, such as mass spectrometry, are required to confirm the identity of this extra band.

PPARγ Agonists Increase Circulating Levels of FGF21 in db/db Mice. FGF21 was among the top five genes, based on degree of regulation, whose mRNA was up-regulated by PPARγ agonists in adipose tissue and annotated as a secreted protein (Table 1). During the preparation of this manuscript, Wang et al. (2008) reported similar results in 3T3-L1 adipocytes. Using anti-FGF21 antibodies, pooled plasma samples from db/db mice were analyzed by Western blot analysis. Interestingly, upon treatment of db/db mice with the PPARγ agonist rosiglitazone, a dose-dependent increase (approximately 3- to 5-fold) in plasma FGF21 was observed, whether only the 23-kDa band or both the 23- and 30-kDa bands were used in the quantitation (Fig. 3). There was either no difference in the plasma concentration of FGF21 between lean db/+ and db/db mice, or there was a decrease in db/db mice compared with lean db/+ mice, depending on whether only the 23-kDa band or both the 23- and 30-kDa bands were used in the quantitation, respectively (Fig. 3).

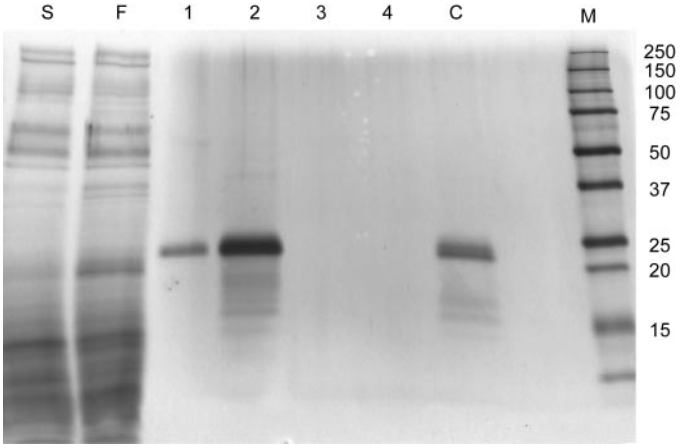

Fig. 2. Purification of mouse FGF21. The *FGF21* gene was expressed in *P. pastoris* as a C-terminal FLAG tag fusion. The protein was purified from the media using anti-Flag column and eluted with FLAG peptide. Eluted material was dialyzed in PBS. Aliquots from different stages of the purification process were analyzed by SDS-PAGE and silver staining. A single protein at the expected size (23 kDa plus FLAG tag) was produced. Lanes are: S, induction supernatant; F, FLAG column flow through; 1–4, FLAG column fractions 1 to 4; C, control FGF21 from a previous preparation; M, Bio-Rad Precision molecular mass markers.

PPARγ Agonists Up-Regulate FGF21 mRNA in Adipose Tissue and Adipocytes but Not in Liver. The transcript for FGF21 was significantly up-regulated in adipose tissue after PPARγ agonist treatment in db/db mice (2.2- and 2.8-fold in EWAT by rosiglitazone and COOH, respectively, both with $p < 0.01$), lean C57BL/6 mice (2.7-fold in EWAT by rosiglitazone with $p < 0.01$), and lean CD1 mice (2.7 and 2.5-fold in EWAT and IWAT, respectively by rosiglitazone with $p < 0.01$). Taqman analysis also confirmed the db/db microarray results (data not shown). We tested several mouse strains and a second fat depot to determine whether the regulation of FGF21 by PPARγ was specific to db/db EWAT or if the response was more general. To further confirm that PPARγ agonists increase FGF21 expression in fat cells, we treated 3T3-L1 adipocytes with rosiglitazone or COOH and observed significant 6.6- and 8.6-fold increases in FGF21 expression, respectively, by microarray analysis (Table 2), in agreement with recent findings (Wang et al., 2008). Examination of liver gene expression of db/db, lean C57BL/6 and 129Sv mice treated with rosiglitazone showed no significant up-regulation of FGF21 mRNA (Table 2). Finally, there was also no difference in FGF21 mRNA levels in EWAT and liver of vehicle treated lean db/+ and db/db mice at baseline. This is consistent with the circulating protein levels if only the 23 kDa immunoreactive band is used to quantitate plasma FGF21 levels (Fig. 3).

PPARα Agonists Regulate FGF21 mRNA Expression Levels in Liver but Not in Adipocytes. The FGF21 transcript was up-regulated in livers of wild-type 129Sv and C57BL/6 mice after treatment with structurally distinct PPARα agonists (3.8 and 4.1-fold by fenofibrate (129Sv) and WY14643 (C57BL/6), respectively, both with $p < 0.01$), and this induction was abolished in PPARα knockout mice (Table 2). In fact, the basal level of this transcript in PPARα KO mice was 5 times lower compared with their wild-type 129Sv littermates (Table 2). These results are consistent with recently published reports (Badman et al., 2007; Inagaki et al., 2007). In terms of adipose tissue, PPARα agonist treatment significantly up-regulated FGF21 mRNA in EWAT of lean C57BL/6 mice (1.7-fold with $p < 0.01$ with WY14643) but had no effect in IWAT of lean CD1 mice (1.1-fold with $p = 0.61$ with fenofibrate) (Table 2). We did not profile each PPARα agonist (WY14643 and fenofibrate) in both adipose depots (EWAT and IWAT) therefore more studies are needed to confirm these results. There was also no effect on FGF21 transcript levels in 3T3-L1 adipocytes after treatment with the PPARα agonist WY14643 (Table 2).

FGF21 Is Up-Regulated by Fasting and High Fat Feeding in Both Liver and Adipose Tissue. In agreement with recently published results (Badman et al., 2007; Inagaki et al., 2007), fasting and high fat diet feeding, both ketogenic conditions, resulted in approximately 1.5- to 3.5-fold increased levels of FGF21 protein in the circulation (Figs. 4 and 5 respectively, depending on which immunoreactive bands are used in the quantitation) and increased levels of FGF21 mRNA in the liver (8.1- and 8.7-fold, respectively, both with $p < 0.01$) (Table 2). The level of FGF21 mRNA in adipose was also increased after fasting and high fat diet feeding, although not as robustly as in liver (2.1- and 1.8-fold, respectively, both with $p < 0.01$) (Table 2).

Discussion

PPARγ regulates the expression of many genes in adipose tissue, either directly or indirectly. Our goal was to assess the transcriptional network regulated by PPARγ and identify potential secreted factors that could influence insulin sensitization. Of the 379 genes robustly regulated by two structurally distinct PPARγ agonists in EWAT of db/db mice, 33 encoded for known secreted proteins. Not surprisingly, a few genes known to be regulated by PPARγ, such as adiponectin (Combs et al., 2002), lipoprotein lipase (Auwerx et al., 1996), laminin β3 (Routh et al., 2002), FGF21 (Wang et al., 2008), and TNFα (Singh Ahuja et al., 2001) were identified. The other genes in Table 1 were not previously associated with PPARγ but are known to be implicated in various pathways such as inflammation, lipid metabolism, and cell growth. These genes could be direct targets of PPARγ or represent downstream secondary effects after treatment with these agents. For example, genes such as Tenascin C (Tnc), ADAM metallopeptidase with thrombospondin type 1 motif 1 (Adamts1), Leucine-rich α-2-glycoprotein 1 (Lrg1), Connective tissue growth factor (Ctgf), Periostin osteoblast specific factor (Postn), and insulin-like growth factor 1 (Igf1) could play a role in cell adhesion and migration. Some gene expression changes could occur because the entire adipose depot was used to isolate RNA and thus effects such as decreased inflammatory cell infiltration could be responsible for the observed changes. Nevertheless, further research is needed to fully understand the significance of the regulation of each of these genes in the context of PPARγ agonism.

At the time of this work, FGF21 was not linked to PPARγ regulation. We focused on FGF21, which is a newly identified molecule with therapeutic potential for diabetes for further follow-up studies (Nishimura et al., 2000; Kharitonenkov et al., 2005, 2007).

The expression of FGF21 in vivo was found to be regulated by PPARγ. The protein was transcriptionally up-regulated in both liver and adipose tissue under a variety of pharmacological and physiological conditions, including fasting and high-fat diet feeding. In the case of PPARγ agonist treatment of db/db mice, mRNA levels for FGF21 were elevated 2- to 3-fold in adipose tissue coincident with an elevation of plasma FGF21 levels. Circulating FGF21 was estimated to be approximately 100 ng/ml in db/db mice and increased up to 500 ng/ml when treated with PPARγ agonists. This estimated increase in circulating FGF21 levels by PPARγ in our experiment is within range with the reported in vitro dosing concentration of 1 μg/ml reported to elicit the insulin sensitization effects in adipocytes (Kharitonenkov et al., 2005). Whether FGF21 plays a role in the insulin sensitization activity of PPARγ agonist is not known, but it is tempting to speculate that PPARγ activation results in an increase in FGF21 production by the adipose tissue, which then acts locally in an autocrine fashion and/or circulates to the liver, muscle, or islets to improve insulin action. In fact, recent evidence suggests that PPARγ agonism enhances the insulin sensitization effects of FGF21 in 3T3-L1 adipocytes and may suggest an amplification of the FGF21 effect to increase glucose uptake in adipose tissue via the increase in FGF21

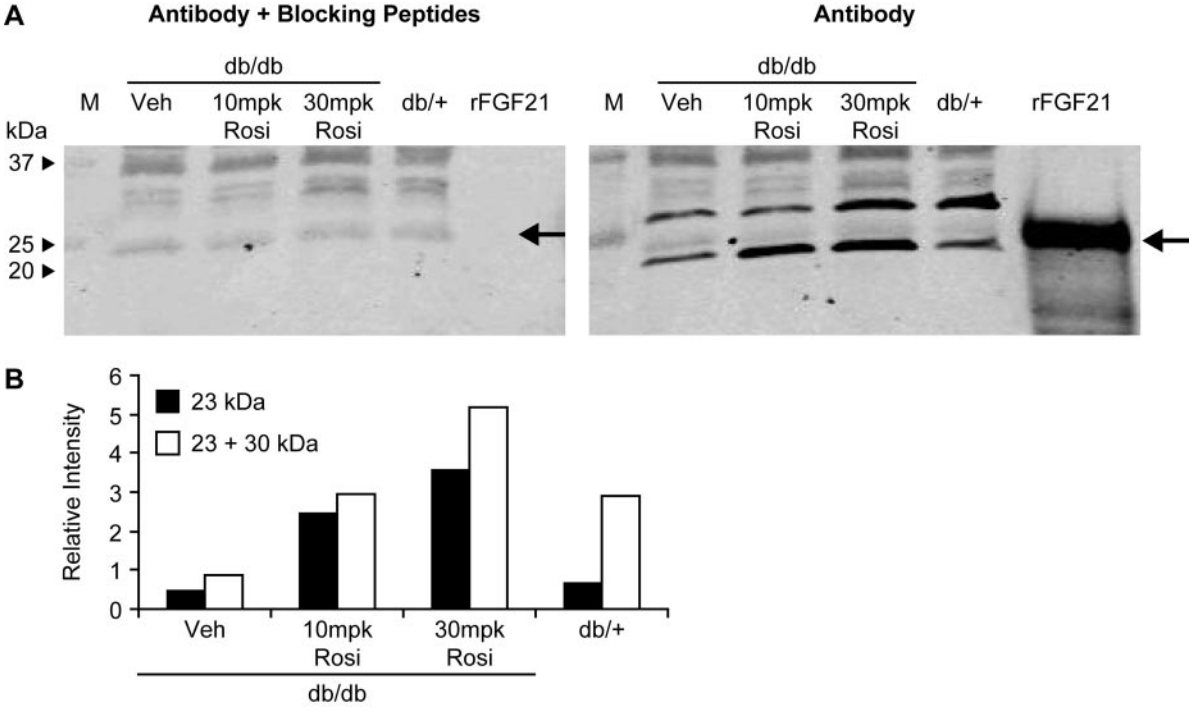

Fig. 3. Plasma FGF21 from db/db mice is up-regulated by the PPARγ agonist rosiglitazone. Immunodetection of pooled plasma from db/db mice treated with rosiglitazone showed an approximately 3- to 5-fold increase in FGF21 protein levels compared with vehicle treatment. Shown in A are representative Western blots with or without pretreatment with blocking peptides showing the immunoreactive 23- and 30-kDa bands representing FGF21. Included on the far right of each blot is recombinant FGF21 protein expressed and purified from *P. pastoris* as a C-terminal flag tag fusion and detected at approximately 25 kDa (arrow). Shown in B is the quantitation of the Western blot in A, right panel, either for the 23-kDa band alone, or the combination of the 23- and 30-kDa bands. Units are relative intensity levels from the densitometer. There was no change in plasma FGF21 between lean db/+ and db/db mice when using only the 23-kDa band, but there was a decrease in db/db compared with lean db/+ mice when using both the 23- and 30-kDa bands.

circulating levels and receptor signaling via an undefined mechanism (Moyers et al., 2007). The fact that FGF21 mRNA was also up-regulated in adipose tissue (EWAT and IWAT) of lean mice (CD1, C57BL/6) after PPARγ agonist treatment suggests that changes in glucose and other metabolites are not regulating FGF21 mRNA levels, because these are not altered by PPARγ agonists in lean animals, and that FGF21 requires some other factor or condition to affect glucose/lipid control.

It is possible that the origin of circulating FGF21 is liver as a result of PPARγ activation in adipose tissue, because FGF21 is normally highly expressed in the liver. However we could not detect any significant up-regulation of FGF21 mRNA in the livers of db/db, C57BL/6, or 129Sv mice after PPARγ agonist treatment. These data suggest that the increase in plasma FGF21 protein after PPARγ agonist treatment is of adipose origin. Consistent with our in vivo findings, Wang et al. (2008) recently reported the identification of PPAR response elements in the promoter region of FGF21 and showed that PPARγ can directly up-regulate this gene in 3T3-L1 adipocytes, further supporting the hypothesis that adipose can secrete FGF21.

Basal expression levels of FGF21 mRNA in adipose and liver of db/db mice were similar to those of lean db/+ mice. This was in agreement with plasma protein levels if only the expected 23-kDa immunoreactive band was used in the quantitation. If both the 23- and 30-kDa bands were used, the circulating FGF21 protein levels would be lower in db/db mice compared with lean db/+ animals, which would be consistent with the decreased insulin sensitivity of this model. But we cannot conclude that the 30-kDa band is indeed FGF21; therefore, we can not draw any conclusion regarding circulating protein levels of FGF21 in lean db/+ versus db/db mice.

Treatment with PPARα agonists up-regulated FGF21 mRNA levels in liver and this was abolished in PPARα knockout mice, consistent with published results (Badman et al., 2007; Inagaki et al., 2007). PPARα agonists also up-regulated FGF21 mRNA in adipose tissue of lean C57BL/6 mice (EWAT) but not that of lean CD1 mice (IWAT) or in 3T3-L1 adipocytes. Additional experiments are needed to confirm the regulation of adipose FGF21 by PPARα.

FGF21 mRNA levels were also significantly up-regulated by fasting and high-fat diet conditions in not only liver, as demonstrated recently (Badman et al., 2007; Inagaki et al., 2007), but also in EWAT of normal mice. In the case of a 24-h fast, liver expression was increased 8.1-fold, whereas adipose expression was increased 2.1-fold (both with $p < 0.01$) (Table

TABLE 2

FGF21 mRNA Expression Summary

Shown are the FGF21 mRNA ratio values obtained by Agilent microarray analysis in the strains and tissues indicated. A ratio greater than 1 signifies up-regulation in the treatment/condition compared to the reference sample (and vice versa). P values were calculated as described under *Materials and Methods*. Normalized intensity values are shown for both the treatment/condition and reference samples. The probe sequence used for FGF21 in the Agilent microarray was CCTGAATCTAGGGCTGTTTCTTTTTGGGTTTCCACTTATTTATTACGGGTATTTATCTTA.

Treatment/Condition: Strain and Tissue	Days	*n*	Reference: Strain and Tissue	Ratio	P	Intensity Treatment	Intensity Reference
Adipose							
db/db EWAT + rosiglitazone, 30 mg/kg	8	3	db/db EWAT + vehicle	2.2	<0.01	0.42	0.19
db/db EWAT + COOH, 30 mg/kg	8	3	db/db EWAT + vehicle	2.8	<0.01	0.59	0.20
db/db EWAT + vehicle	8	3	db/db EWAT + vehicle	0.9	0.01	0.17	0.20
db/db EWAT + vehicle	8	3	db/+ EWAT + vehicle	1.1	0.03	0.14	0.12
db/+ EWAT + vehicle	8	3	db/+ EWAT + vehicle	1.0	0.68	0.13	0.13
C57BL/6 EWAT + rosiglitazone, 100 mg/kg	7	3	C57BL/6 EWAT + vehicle	2.7	<0.01	0.46	0.16
C57BL/6 EWAT + WY14643, 30 mg/kg	7	3	C57BL/6 EWAT + vehicle	1.7	<0.01	0.31	0.17
C57BL/6 EWAT + vehicle	7	3	C57BL/6 EWAT + vehicle	1.1	0.50	0.18	0.15
CD1 EWAT + rosiglitazone, 100 mg/kg	14	3	CD1 EWAT + vehicle, 14 days	2.7	<0.01	1.26	0.42
CD1 EWAT + vehicle	14	3	CD1 EWAT + vehicle, 14 days	1.1	0.43	0.40	0.35
CD1 IWAT + rosiglitazone, 100 mg/kg	14	3	CD1 IWAT + vehicle, 14 days	2.5	<0.01	0.15	0.40
CD1 IWAT + fenofibrate 300 mg/kg	14	3	CD1 IWAT + vehicle, 14 days	1.1	0.61	0.12	0.14
CD1 IWAT + vehicle	14	3	CD1 IWAT + vehicle, 14 days	1.0	0.85	0.18	0.18
3T3-L1 Adipocytes + rosiglitazone, 10 μM		2	3T3-L1 Adipocytes + vehicle	6.6	<0.01	0.44	0.07
3T3-L1 Adipocytes + COOH, 10 μM		2	3T3-L1 Adipocytes + vehicle	8.6	<0.01	0.54	0.06
3T3-L1 Adipocytes + WY14643, 10 μM		2	3T3-L1 Adipocytes + vehicle	1.0	0.89	0.06	0.06
3T3-L1 Adipocytes + vehicle		3	3T3-L1 Adipocytes + vehicle	1.0	0.58	0.06	0.05
C57BL/6 EWAT + fast	1	4	C57BL/6 EWAT + chow	2.1	<0.01	0.65	0.29
C57BL/6 EWAT + HFD	70	4	C57BL/6 EWAT + chow	1.8	<0.01	0.62	0.32
C57BL/6 EWAT + chow		4	C57BL/6 EWAT + chow	1.0	0.71	0.27	0.26
Liver							
129Sv Liver + fenofibrate, 200 mg/kg	7	3	129Sv Liver + vehicle	3.8	<0.01	2.52	0.66
129Sv Liver + rosiglitazone, 100 mg/kg	7	3	129Sv Liver + vehicle	0.8	0.12	0.48	0.59
129Sv Liver + vehicle	7	3	129Sv Liver + vehicle	1.0	0.96	0.62	0.59
129Sv PPARαKO Liver + fenofibrate, 200 mg/kg	7	3	129Sv PPARαKO Liver + vehicle	1.0	0.78	0.12	0.13
129Sv PPARαKO Liver + rosiglitazone, 100 mg/kg	7	3	129Sv PPARαKO Liver + vehicle	1.2	0.22	0.11	0.10
129Sv PPARαKO Liver + vehicle	7	3	129Sv Liver + vehicle	0.2	<0.01	0.17	0.77
C57BL/6 Liver + rosiglitazone, 100 mg/kg	7	3	C57BL/6 Liver + vehicle	1.2	0.32	0.30	0.25
C57BL/6 Liver + WY14643, 30 mg/kg	7	3	C57BL/6 Liver + vehicle	4.1	<0.01	1.27	0.26
C57BL/6 Liver + vehicle	7	3	C57BL/6 Liver + vehicle	1.0	0.82	0.27	0.29
db/db Liver + rosiglitazone, 30 mg/kg	8	3	db/db Liver + vehicle	1.2	0.26	0.24	0.20
db/db Liver + vehicle	8	3	db/db Liver + vehicle	0.8	0.29	0.21	0.23
db/db Liver + vehicle	8	5	db/+ Liver + vehicle	0.9	0.39	0.54	0.58
C57BL/6 Liver + fast	1	4	C57BL/6 Liver + chow	8.1	<0.01	4.66	0.45
C57BL/6 Liver + HFD	70	4	C57BL/6 Liver + chow	8.7	<0.01	3.05	0.34
C57BL/6 Liver + chow		4	C57BL/6 Liver + chow	0.9	0.67	0.32	0.34

HFD, high-fat diet.

2). The gene expression changes were substantiated by increases in plasma protein levels as high as approximately 3-fold (Fig. 4). A similar effect was observed under 10 weeks of high-fat feeding conditions; liver and adipose gene expressions were up 8.7- and 1.8-fold, respectively (both with $p < 0.01$, Table 2), and plasma protein levels were increased up to approximately 3.5-fold (Fig. 5).

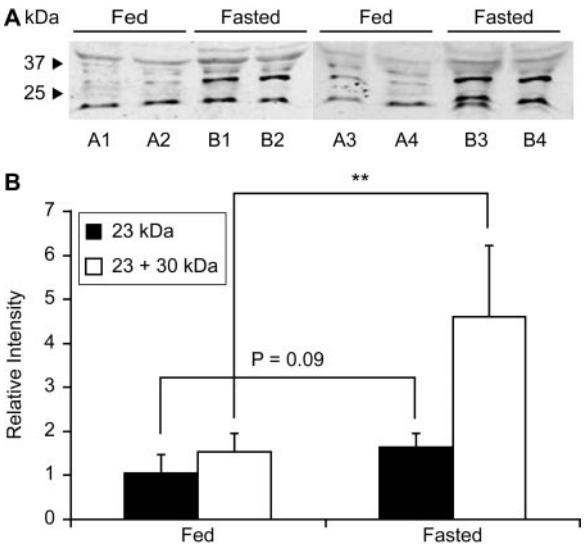

Fig. 4. Plasma FGF21 is increased upon fasting. C57BL/6 mice were fasted for 48 h, and plasma was collected and analyzed by Western blot relative to fed mice. The fasted cohort (B1–4) exhibited an increase in immunopositive bands (at 23- and 30-kDa) compared with the fed cohort (A1–4) (A). Shown in B are the quantitation of either the 23-kDa band alone or the 23- + 30-kDa bands together by densitometry showing a 1.5- (not significant) and 3-fold increase of plasma FGF21 with fasting, respectively. Data are expressed as mean ± S.D. Statistical analysis was performed by the Student's *t* test (two-sample, two-tail) to determine whether there were significant differences between the diets. **, $P < 0.01$.

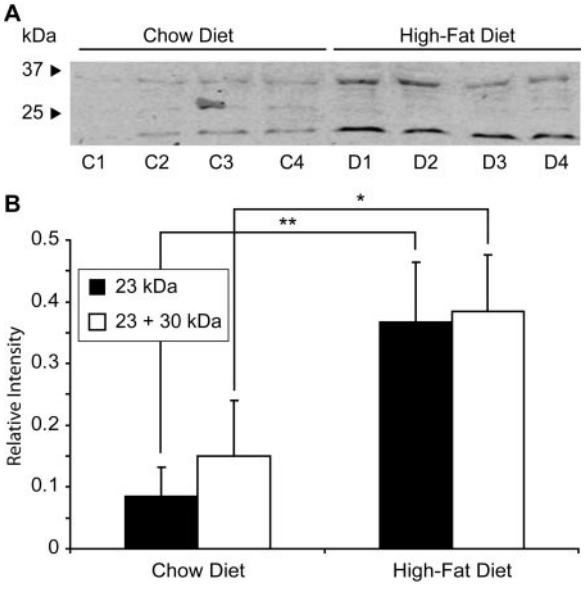

Fig. 5. Plasma FGF21 is increased on high-fat diet. C57BL/6 mice were fed a high-fat diet for 4 weeks and plasma samples were collected and analyzed by Western blot relative to chow fed mice. The high-fat diet cohort (D1–4) exhibited an increase in immunopositive bands (at 23- and 30-kDa) compared with the chow diet cohort (C1–4) (A). Shown in B are the quantitation of either the 23-kDa band alone or the 23- + 30-kDa bands together by densitometry showing an approximately 3.5- and 2.5-fold increase of plasma FGF21 with high-fat diet feeding, respectively. Data are expressed as mean ± S.D. Statistical analysis was performed by the Student's *t* test (two-sample, two-tail) to determine whether there were significant differences between the diets. **, $P < 0.01$; *, $P < 0.05$.

In conclusion, we have used transcriptional profiling to identify 33 genes coding for secreted proteins that were robustly regulated by PPARγ agonists in adipose tissue of diabetic db/db mice. Several have previously been implicated in the diabetes phenotype (glucose and lipid metabolism and inflammation). Here, FGF21 was further characterized in terms of mRNA and protein expression regulation across several pharmacological and metabolic perturbations, including fasting and high-fat diet feeding. Although FGF21 was recently reported to be regulated by PPARα agonists in liver and by PPARγ agonists in an adipocytic cell line, we show that this protein is regulated by PPARγ agonists in adipose tissue in vivo and circulates in the plasma. We also report the first soluble expression of recombinant FGF21 using the *P. pastoris* expression system, and this will be useful in future biochemical analysis of this very interesting protein. Other genes in this list were described previously to be regulated by PPARγ and have been implicated in the molecular pathway of this transcription factor. The identification of novel PPARγ-regulated genes enhances our knowledge of the mechanisms of action of this master regulator and could point to novel drug targets for the metabolic syndrome.

Acknowledgments

We thank Tomas Doebber, Margaret Wu, and Roger Meurer for the db/db, PPARα KO, and CD1 animal studies; Ching Chang and Margaret McCann for the C57BL/6 PPAR agonist study; Marie Thompson and Gino Castriota for the 3T3-L1 PPARγ agonist study; Merck Research Laboratory chemists for synthesizing rosiglitazone, COOH, and fenofibrate; Robert Kleinhanz, Mark Ferguson, and Michelle Thorton for project management; Ruojing Wang for critical reading of the manuscript; and the Rosetta Gene Expression Laboratory for the microarray processing.

References

Allan CM and Taylor JM (1996) Expression of a novel human apolipoprotein (apoC-IV) causes hypertriglyceridemia in transgenic mice. *J Lipid Res* **37:**1510–1518.
Auwerx J, Schoonjans K, Fruchart JC, and Staels B (1996) Transcriptional control of triglyceride metabolism: fibrates and fatty acids change the expression of the LPL and apo C-III genes by activating the nuclear receptor PPAR. *Atherosclerosis* **124:**S29–S37.
Badman MK, Pissios P, Kennedy AR, Koukos G, Flier JS, and Maratos-Flierl E (2007) Hepatic fibroblast growth factor 21 is regulated by PPAR alpha and is a key mediator of hepatic lipid metabolism in ketotic states. *Cell Metabolism* **5:**426–437.
Berger JP, Akiyama TE, and Meinke PT (2005) PPARs: therapeutic targets for metabolic disease. *Trends Pharmacol Sci* **26:**244–251.
Blagoev B, Kratchmarova I, Nielsen MM, Fernandez MM, Voldby J, Andersen JS, Kristiansen K, Pandey A, and Mann M (2002) Inhibition of adipocyte differentiation by resistin-like molecule α- biochemical characterization of its oligomeric nature. *J Biol Chem* **277:**42011–42016.
Boyle PJ (2004) What are the effects of peroxisome proliferator-activated receptor agonists on adiponectin, tumor necrosis factor-alpha, and other cytokines in insulin resistance? *Clin Cardiol* **27:**11–16.
Carley AN, Semeniuk LM, Shimoni Y, Aasum E, Larsen TS, Berger JP, and Severson DL (2004) Treatment of type 2 diabetic db/db mice with a novel PPAR gamma agonist improves cardiac metabolism but not contractile function. *Am J Physiol Endocrinol Metab* **286:**E449–E455.
Combadiere C, Ahuja SK, Vandamme J, Tiffany HL, Gao JL, and Murphy PM (1995) Monocyte chemoattractant protein-3 is a functional ligand for CC chemokine receptor-1 and receptor-2B. *J Biol Chem* **270:**29671–29675.
Combs TP, Wagner JA, Berger J, Doebber T, Wang WJ, Zhang BB, Tanen M, Berg AH, O'Rahilly S, Savage DB, et al. (2002) Induction of adipocyte complement-related protein of 30 kilodaltons by PPAR gamma agonists: a potential mechanism of insulin sensitization. *Endocrinology* **143:**998–1007.
Hata H, Sakaguchi N, Yoshitomi H, Iwakura Y, Sekikawa K, Azuma Y, Kanai C, Moriizumi E, Nomura T, Nakamura T, et al. (2004) Distinct contribution of IL-6, TNF-alpha, IL-1, and IL-10 to T cell-mediated spontaneous autoimmune arthritis in mice. *J Clin Invest* **114:**582–588.
Heinemann A, Hartnell A, Stubbs VEL, Murakami K, Soler D, LaRosa G, Askenase PW, Williams TJ, and Sabroe I (2000) Basophil responses to chemokines are

regulated by both sequential and cooperative receptor signaling. *J Immunol* **165:** 7224–7233.
Hughes TR, Mao M, Jones AR, Burchard J, Marton MJ, Shannon KW, Lefkowitz SM, Ziman M, Schelter JM, Meyer MR, et al. (2001) Expression profiling using microarrays fabricated by an ink-jet oligonucleotide synthesizer. *Nat Biotechnol* **19:**342–347.
Inagaki T, Dutchak P, Zhao GX, Ding XS, Gautron L, Parameswara V, Li Y, Goetz R, Mohammadi M, Esser V, et al. (2007) Endocrine regulation of the fasting response by PPAR alpha-mediated induction of fibroblast growth factor 21. *Cell Metab* **5:**415–425.
Jadus MR, Irwin MCN, Irwin MR, Horansky RD, Sekhon S, Pepper KA, Kohn DB, and Wepsic HT (1996) Macrophages can recognize and kill tumor cells bearing the membrane isoform of macrophage colony-stimulating factor. *Blood* **87:**5232–5241.
Kharitonenkov A, Shiyanova TL, Koester A, Ford AM, Micanovic R, Galbreath EJ, Sandusky GE, Hammond LJ, Moyers JS, Owens RA, et al. (2005) FGF-21 as a novel metabolic regulator. *J Clin Invest* **115:**1627–1635.
Kharitonenkov A, Wroblewski VJ, Koester A, Chen YF, Clutinger CK, Tigno XT, Hansen BC, Shanafelt AB, and Etgen GJ (2007) The metabolic state of diabetic monkeys is regulated by fibroblast growth factor-21. *Endocrinology* **148:**774–781.
Kimura A, Baumann CA, Chiang SH, and Saltiel AR (2001) The sorbin homology domain: a motif for the targeting of proteins to lipid rafts. *Proc Natl Acad Sci U S A* **98:**9098–9103.
Klimcakova E, Moro C, Mazzucotelli A, Lolmede K, Viguerie N, Galitzky J, Stich V, and Langin D (2007) Profiling of adipokines secreted from human subcutaneous adipose tissue in response to PPAR agonists. *Biochem Biophys Res Commun* **358:**897–902.
Koishi R, Ando Y, Ono M, Shimamura M, Yasumo H, Fujiwara T, Horikoshi H, and Furukawa H (2002) Angptl3 regulates lipid metabolism in mice. *Nature Genetics* **30:**151–157.
Kretowski A, Mysliwiec J, and Kinalska I (2000) In vitro interleukin-13 production by peripheral blood in patients with newly diagnosed insulin-dependent diabetes mellitus and their first degree relatives. *Scand J Immunol* **51:**321–325.
Laplante M, Festuccia WT, Soucy G, Gelinas Y, Lalonde J, Berger JP, and Deshaies Y (2006) Mechanisms of the depot specificity of peroxisome proliferator-activated receptor gamma action on adipose tissue metabolism. *Diabetes* **55:**2771–2778.
Lecka-Czernik B, Ackert-Bicknell C, Adamo ML, Marmolejos V, Churchill GA, Shockley KR, Reid IR, Grey A, and Rosen CJ (2007) Activation of peroxisome proliferator-activated receptor gamma (PPAR gamma) by rosiglitazone suppresses components of the insulin-like growth factor regulatory system in vitro and in vivo. *Endocrinology* **148:**903–911.
Lee SST, Pineau T, Drago J, Lee EJ, Owens JW, Kroetz DL, Fernandezsalguero PM, Westphal H, and Gonzalez FJ (1995) Targeted disruption of the alpha-isoform of the peroxisome proliferator-activated receptor gene in mice results in abolishment of the pleiotropic effects of peroxisome proliferators. *Mol Cell Biol* **15:**3012–3022.
Lloyd GM, Minto AW, Dorf ME, Proudfoot A, Wells TNC, Salant DJ, and GutierrezRamos JC (1997) RANTES and monocyte chemoattractant protein-1 (MCP-1) play an important role in the inflammatory phase of crescentic nephritis, but only MCP-1 is involved in crescent formation and interstitial fibrosis. *J Exp Med* **185:**1371–1380.
Moore BB, Murray L, Das A, Wilke CA, Herrygers AB, and Toews GB (2006) The role of CCL12 in the recruitment of fibrocytes and lung fibrosis. *Am J Respir Cell Mol Biol* **35:**175–181.
Moyers JS, Shiyanova TL, Mehrbod F, Dunbar JD, Noblitt TW, Otto KA, Reifel-Miller A, and Kharitonenkov A (2007) Molecular determinants of FGF-21 activity-synergy and cross-talk with PPAR gamma signaling. *J Cell Physiol* **210:**1–6.
Nawrocki AR, Rajala MW, Tomas E, Pajvani UB, Saha AK, Trumbauer ME, Pang Z, Chen AS, Ruderman NB, Chen H, et al. (2006) Mice lacking adiponectin show decreased hepatic insulin sensitivity and reduced responsiveness to peroxisome proliferator-activated receptor gamma agonists. *J Biol Chem* **281:**2654–2660.
Nishimura T, Nakatake Y, Konishi M, and Itoh N (2000) Identification of a novel FGF, FGF-21, preferentially expressed in the liver. *Biochim Biophys Acta* **1492:** 203–206.
Rokudai A, Terui Y, Kuniyoshi R, Mishima Y, Mishima Y, Aizu-Yokota E, Sonoda Y, Kasahara T and Hatake K (2006) Differential regulation of eotaxin-1/CCL11 and eotaxin-3/CCL26 production by the TNF-alpha and IL-4 stimulated human lung fibroblast. *Biol Pharm Bull* **29:**1102–1109.
Routh RE, Johnson JH, and McCarthy KJ (2002) Troglitazone suppresses the secretion of type i collagen by mesangial cells in vitro. *Kidney Int* **61:**1365–1376.
Scherer PE, Williams S, Fogliano M, Baldini G, and Lodish HF (1995) A novel serum-protein similar to C1Q, produced exclusively in adipocytes. *J Biol Chem* **270:**26746–26749.
Singh Ahuja H, Liu S, Crombie DL, Boehm M, Leibowitz MD, Heyman RA, Depre C, Nagy L, Tontonoz P, and Davies PJA (2001) Differential effects of rexinoids and thiazolidinediones on metabolic gene expression in diabetic rodents. *Mol Pharmacol* **59:**765–773.
Steppan CM, Bailey ST, Bhat S, Brown EJ, Banerjee RR, Wright CM, Patel HR, Ahima RS, and Lazar MA (2001) The hormone resistin links obesity to diabetes. *Nature* **409:**307–312.
Teshima S, Rokutan K, Nikawa T, and Kishi K (1998) Macrophage colony-stimulating factor stimulates synthesis and secretion of a mouse homolog of a human ige-dependent histamine-releasing factor by macrophages in vitro and in vivo. *J Immunol* **161:**6356–6366.
Wang H, Qiang L and Farmer SR (2008) Identification of a domain within PPAR{gamma} regulating expression of a group of genes containing FGF21 that are selectively repressed by SIRT1 in adipocytes. *Mol Cell Biol* **28:**188–200.
Wild S, Roglic G, Green A, Sicree R, and King H (2004) Global prevalence of diabetes—estimates for the year 2000 and projections for 2030. *Diabetes Care* **27:**1047–1053.
Woods SC, Seeley RJ, Porte D, and Schwartz MW (1998) Signals that regulate food intake and energy homeostasis. *Science* **280:**1378–1383.
Yakar S, Setser J, Zhao H, Stannard B, Haluzik M, Glatt V, Bouxsein ML, Kopchick JJ, and LeRoith D (2004) Inhibition of growth hormone action improves insulin sensitivity in liver IGF-1-deficient mice. *J Clin Invest* **113:**96–105.
Yu JG, Javorschi S, Hevener AL, Kruszynska YT, Norman RA, Sinha M, and Olefsky JM (2002) The effect of thiazolidinediones on plasma adiponectin levels in normal, obese, and type 2 diabetic subjects. *Diabetes* **51:**2968–2974.
Zhang B, Berger J, Hu EI, Szalkowski D, WhiteCarrington S, Spiegelman BM, and Moller DE (1996) Negative regulation of peroxisome proliferator-activated receptor-gamma gene expression contributes to the antiadipogenic effects of tumor necrosis factor-alpha. *Mol Endocrinol* **10:**1457–1466.

Address correspondence to: Kenny K. Wong, Merck Research Laboratories, P.O. Box 2000, Rahway, NJ 07065, USA. E-mail: kenny_wong@merck.com